



Universidad Autónoma  
de Madrid

**Biblos-e Archivo**  
Repositorio Institucional UAM

**Repositorio Institucional de la Universidad Autónoma de Madrid**

<https://repositorio.uam.es>

Esta es la **versión de autor** del artículo publicado en:  
This is an **author produced version** of a paper published in:

Angewandte Chemie International Edition 59.39 (2020): 17091-17096

**DOI:** <https://doi.org/10.1002/anie.202006877>

**Copyright:** © 2020 Wiley-VCH Verlag GmbH & Co. KGaA, Weinheim

El acceso a la versión del editor puede requerir la suscripción del recurso

Access to the published version may require subscription

# Nanostructured Micelle Nanotubes Self-assembled from Dinucleobase Monomers in Water

Fátima Aparicio,<sup>[a]</sup> Paula B. Chamorro,<sup>[a]</sup> Raquel Chamorro,<sup>[a]</sup> Santiago Casado,<sup>[b]</sup> and David González-Rodríguez<sup>[a,c]\*</sup>

[a] Dr. F. Aparicio, P. B. Chamorro, Dr. R. Chamorro, Prof. D. González-Rodríguez  
Nanostructured Molecular Systems and Materials (MSMn) Group, Departamento de Química Orgánica, Facultad de Ciencias  
Universidad Autónoma de Madrid, 28049 Madrid, Spain  
E-mail: [david.gonzalez.rodriguez@uam.es](mailto:david.gonzalez.rodriguez@uam.es)

[b] Dr. S. Casado  
IMDEA Nanociencia,  
c/ Faraday 9, Campus de Cantoblanco, 28049, Madrid, Spain

[c] Prof. D. González-Rodríguez  
Institute for Advanced Research in Chemical Sciences (IAdChem)  
Universidad Autónoma de Madrid, 28049 Madrid, Spain

Supporting information for this article is given via a link at the end of the document.

**Abstract:** Despite the central importance of aqueous amphiphile assemblies in science and industry, the size and shape of these nano-objects is often difficult to control with accuracy due to the non-directional nature of the hydrophobic interactions that sustain them. Here, using a bioinspired strategy that consists in programming an amphiphile with shielded directional Watson-Crick hydrogen-bonding functions, we managed to guide its self-assembly in water toward a novel family of chiral micelle nanotubes with partially filled lipophilic pores of about 2 nm in diameter. Moreover, we successfully demonstrate that these tailored nanotubes are able to extract and host molecules that are complementary in size and chemical affinity.

## Introduction

Water is the essential environment for all biological assembly processes and molecular recognition events. It is therefore not surprising to see that supramolecular chemistry is increasingly evolving to aqueous spaces and connecting with biochemistry targets and tools.<sup>[1]</sup> However, the design rules for synthetic assemblies change substantially when moving from the classical organic to aqueous media.<sup>[2]</sup> In the former, well-defined objects are created by using noncovalent motifs that are *enthalpically strong* and highly directional, like metal-ligand or hydrogen(H)-bonding interactions. Water, on the contrary, is a polar molecule and a strong H-bonding donor and acceptor, and competes severely with such interactions. Instead, self-assembly in water has been classically dominated by exploiting the *hydrophobic effect*, which contains a favorable *entropic contribution* due to the preference of water for sustaining its own H-bonded network, where apolar moieties are excluded. This is the basis of the organization of amphiphilic molecules (*i.e.* surfactants) in high order structures of enormous importance in biological membranes and synthetic systems for food, cosmetics or healthcare industries. However, the low directionality of hydrophobic interactions hampers a precise control of supramolecular structure, and classical aqueous assemblies comprise micelles or vesicles, whose size and shape (*i.e.* spherical, cylindrical, lamellar) is often difficult to predict with (subnanometer) accuracy.<sup>[3]</sup> In order to accomplish strict structural control, natural systems make use of

a strategy that is based on shielding directional interactions into hydrophobic pockets, so that they are forced to interact complementarily, as illustrated in DNA assembly or protein folding.

Following this bioinspired strategy, we aim in this work at reaching a precise control on the shape and dimensions of amphiphilic assemblies, so as to build unique architectures in aqueous environments. In particular, by programming an amphiphile with directional and complementary hydrogen-bonding interactions, we managed to synthesize a novel class of helically chiral nanotubes with structurally defined pores that can be tailored with lipophilic chemical coatings (Figure 1), as in micellar architectures.

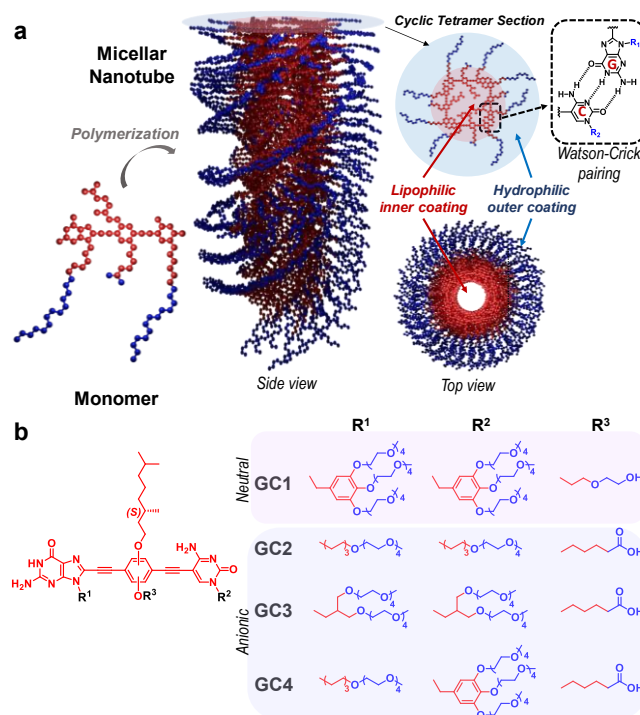


**Figure 1.** (a) Scheme of the two-step self-assembly of **GC2** monomers into nanotubes. (b) Chemical structure of the amphiphilic **GC1-GC4** dinucleobase derivatives. Hydrophobic and hydrophilic parts are represented in red and blue, respectively.

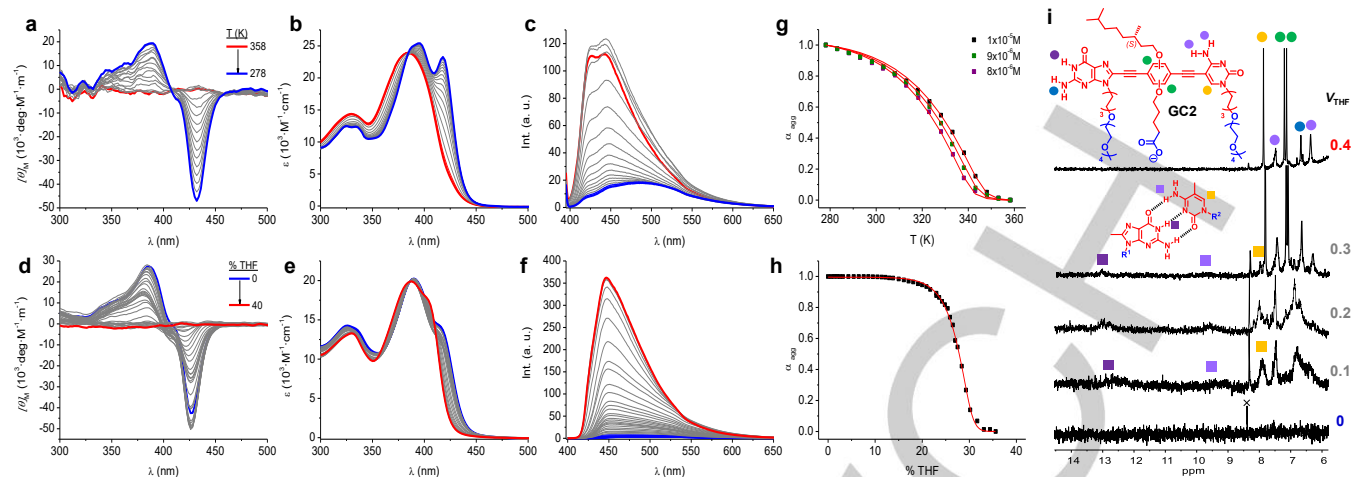


**Figure 2.** (a,d) CD, (b,e) absorption and (c,f) emission spectral changes recorded for **GC2** as a function of (a-c) temperature (in Milli-Q H<sub>2</sub>O;  $1.0 \cdot 10^{-5}$  M) or (d-f) solvent composition in THF-H<sub>2</sub>O mixtures (298 K;  $2.0 \cdot 10^{-4}$  M). (g) Temperature- and (h) solvent-dependent curves obtained from (g) the UV-vis data at 3 concentrations or (h) the emission data, and fitted to the corresponding nucleation-elongation models (red lines). (i) Structure of compound **GC2** and <sup>1</sup>H NMR spectra acquired at different H<sub>2</sub>O:THF-D<sub>8</sub> compositions (298 K;  $2.0 \cdot 10^{-4}$  M). Circles and squares indicate respectively protons in the monomer and aggregated forms.

Interestingly, this unprecedented design produced tubular structures with uniform, partially filled pores of about 2 nm, which are compatible with molecular dimensions and thus allows to fill the gap between nanotubes generated through the stacking of covalent macrocycles,<sup>[4]</sup> rosettes,<sup>[5]</sup> or foldamers,<sup>[6]</sup> with typical pore diameters below 1 nm, and the nanotubes assembled from classical amphiphilic molecules, with internal diameters exceeding 10 nm.<sup>[7]</sup>

## Results and Discussion

In order to precisely rule nanotube diameter and inner pore structure, we made use of a high-fidelity supramolecular cyclotetramerization process by Watson-Crick pairing<sup>[8]</sup> of  $\pi$ -conjugated rod-like monomers substituted at the edges by complementary nucleobases (in this case, guanine (G) and cytosine (C)), as recently studied by us in organic solvents.<sup>[9]</sup> We made, nonetheless, a few structural modifications to adapt these systems to aqueous environments (Figure 1b). First, oligo(ethyleneglycol) (OEG) tails were attached at the *N*-1/*N*-9 positions of the C/G bases to improve solubility in the final assemblies. Besides, in order to protect Watson-Crick pairing, hydrophobic alkyl/benzyl segments were added to these tails in the region close to the heterocyclic cores. Second, an amphiphilic *p*-phenylene block was installed between the bases, equipped with a *S*-chiral lipophilic chain on one side, to provide helically chiral assemblies, and a hydrophilic neutral (alcohol) or ionic (carboxylate) tail on the other. During self-assembly, we expect that all hydrophobic moieties that don't show affinity for the aqueous environment will be forced to group within the tube pore, thus exposing the hydrophilic tails to the external medium. Such design would yield a nanostructured tubular micelle with a disk-like section comprising a hydrophilic outer region and a hydrophobic core, as schematically represented in Figure 1a.

Keeping this general molecular design, we synthesized a series of dinucleobase derivatives having small structural variations so as to determine the most important elements that contribute to: 1) enhance water solubility, 2) promote nanotube

formation, and 3) afford high reproducibility and reliability, not only in the supramolecular process, but also along the synthetic routes. Such variations are schematically represented in Figure 1b, and basically include: a) the number of OEG tails and the nature of the lipophilic segment connected to *N*-1/*N*-9 at the C/G bases, and b) the neutral/ionic nature of the hydrophilic chain attached to the central block. Compound structure (Figure S1) and all synthetic details (Section S1) can be found at the S.I.

All monomers were then subjected to preliminary spectroscopy (<sup>1</sup>H NMR, absorption, emission and CD) and microscopy (AFM, TEM) studies. As further detailed in the S.I. (Figures S2A-N), all peripheral groups installed in the monomers were able to afford solubility in water at concentrations below  $10^{-3}$  M, and to induce aggregation at room temperature into CD-active objects with the expected morphology and dimensions. The only exception was **GC3**, endowed with di-OEG tails at both bases, which showed a higher resistance to aggregation. We presume that this is due to the fact that this group, having a rather short hydrophobic segment, does not supply sufficient shielding for Watson-Crick pairing. This preliminary screening allowed us to select compound **GC2**, shown also in Figure 2, as the best suited monomer in terms of the conditions 1-3 listed above, so it was subjected to a deeper supramolecular study.

Thus, when dissolved in neutral/buffered water (pH = 5-9) at concentrations between  $6.0 \cdot 10^{-4}$  and  $1.0 \cdot 10^{-6}$  M, **GC2** displayed spectroscopic features that are stable for weeks and consistent with a chirally organized supramolecular structure (blue spectra in Figures 2a-f), which can be disassembled by increasing temperature or the volume fraction of a denaturing solvent, like THF or MeOH (red spectra in Figures 2a-f). This process is reversible, and the spectral characteristics of the **GC2** assemblies can be restored upon cooling or increasing water content, revealing virtually the same trends and therefore excluding the presence of kinetic intermediates. Such association process can be monitored by: 1) the recovery of the original CD signal, displaying a negative Cotton effect (Figures 2a,d); 2) the growth of a red-shifted absorption band at 418 nm (Figures 2b,e); and 3) a notable red shift (from 434 to 488 nm) and decrease in emission intensity (Figures 2c,f). It should be remarked that these spectral changes are very similar to the ones recorded along the



**Table 1.** Thermodynamic parameters calculated for **GC2** upon (a) polymerization by decreasing temperature, and (b) depolymerization by increasing  $V_{\text{THF}}$ .

		$K_n$ ( $\text{M}^{-1}$ ) <sup>[a]</sup>	$K_e$ ( $\text{M}^{-1}$ ) <sup>[b]</sup>	$\sigma$ <sup>[c]</sup>	$\Delta H^0$ ( $\text{KJ/mol}$ ) <sup>[d]</sup>	$\Delta S^0$ ( $\text{J/mol}\cdot\text{K}$ ) <sup>[e]</sup>	$\Delta H_n^0$ ( $\text{KJ/mol}$ ) <sup>[f]</sup>	$m$ ( $\text{KJ/mol}$ ) <sup>[g]</sup>	$\Delta G$ ( $\text{KJ/mol}$ ) <sup>[h]</sup>
<b>a</b>	$\text{H}_2\text{O}$ <sup>[i]</sup>	$4.1\cdot 10^2$	$9.3\cdot 10^5$	$4.4\cdot 10^{-4}$	$-40.6 \pm 0.9$	$-21.9 \pm 2.8$	$-19.2 \pm 0.8$	-	-
	$\text{H}_2\text{O}/\text{THF}$ <sup>[k]</sup>	$4.3\cdot 10^2$	$2.0\cdot 10^4$	$2.1\cdot 10^{-2}$	$-66.0 \pm 1.7$	$-139.2 \pm 5.5$	$-9.5 \pm 0.4$	-	-
<b>b</b>	$\text{H}_2\text{O} + \text{THF}$ <sup>[l]</sup>	-	-	$0.56 \pm 0.05$	-	-	-	$86.6 \pm 4.9$	$-49.8 \pm 1.6$

[a] Nucleation and [b] elongation constants, [c] degree of cooperativity, elongation [d] enthalpy and [e] entropy, and nucleation [f] enthalpy of the polymerization process calculated by decreasing  $T$ . [g]  $m$  Parameter, [h] Gibbs free energy, and [i] degree of cooperativity of the depolymerization process observed by increasing  $V_{\text{THF}}$ . [j] Global fitting from solutions at  $1.0\cdot 10^{-5}$ ,  $9.0\cdot 10^{-6}$  and  $8.0\cdot 10^{-6}$  M. [k] Cooling process at  $V_{\text{THF}} = 0.2$  and  $2.0\cdot 10^{-4}$  M. [l] Performed at  $2.0\cdot 10^{-4}$  M.

cyclization<sup>[9a]</sup> and polymerization<sup>[9g]</sup> processes of related lipophilic dinucleobase monomers in organic solvents, which preliminarily suggests that the **GC2** assemblies are constituted by the corresponding  $c(\text{GC2})_4$  cyclic units.

The CD, absorption and emission trends obtained by varying temperature (Figure S3A) or solvent composition (Figure S3C) revealed non-sigmoidal curves that are consistent with cooperative polymerization processes and that could be quantitatively analyzed with appropriate models (see also S.I.). First, the cooling curves recorded at 3 different concentrations were globally fitted to a nucleation-elongation model (Figure 2g),<sup>[10]</sup> which allowed to obtain a set of thermodynamic parameters (Table 1) including: the elongation enthalpy ( $\Delta H^0$ ) and entropy ( $\Delta S^0$ ), the nucleation enthalpy ( $\Delta H_n^0$ ), the nucleation ( $K_n$ ) and elongation ( $K_e$ ) equilibrium constants and, finally, the degree of cooperativity ( $\sigma$ ) associated with the polymerization process, calculated as:  $\sigma = K_n/K_e$ . The low  $\sigma$  value determined highlights a highly favorable elongation process in the supramolecular polymerization of **GC2** compared to the nucleation step. Likewise, the depolymerization process was monitored by these three spectroscopic techniques by gradually increasing the volume fraction of THF ( $V_{\text{THF}}$ ) in water-THF mixtures, and fitted to the corresponding nucleation-elongation model (Figure 2h),<sup>[11]</sup> which allows to determine the Gibbs free energy gain upon monomer addition ( $\Delta G^0$ ), as well as the degree of cooperativity ( $\sigma$ ). As can be noted in Table 1, the  $\sigma$  factors calculated in these two experiments differ considerably, in about 3 orders of magnitude, but this is not surprising since the experimental conditions are totally different. To ascertain the role of THF in the polymerization cooperativity, we also analyzed cooling curves with diverse proportions of this denaturing solvent (see Figure S3D as an example). The spectral changes recorded are virtually identical to those seen in pure water but, as shown in Table 1 at  $V_{\text{THF}} = 0.2$ , the degree of cooperativity is reduced in the presence of THF.

In order to get a deeper insight into this supramolecular process and to gather some evidence for G:C Watson-Crick pairing in the assembled state, we made  $^1\text{H}$  NMR experiments at different  $\text{H}_2\text{O}:\text{THF}-D_8$  compositions (Figure 2i). As expected, **GC2** in water shows extremely broad proton signals that produce a flat  $^1\text{H}$  NMR spectrum, which is consistent with the formation of large aggregates. At  $V_{\text{THF}} = 0.4$ , in contrast, the spectrum reveals sharp signals for each proton, which indicates that **GC2** is molecularly dissolved, in agreement with all other spectroscopic techniques. However, at intermediate  $V_{\text{THF}}$ , aggregated species can be detected in slow NMR exchange with the monomer that show typical  $^1\text{H}$  signals for G:C pairing, with H-bonded G-amide and C-amine protons at around 13.0 and 9.5 ppm. Although this result resembles what we observed along the cyclotetramerization

process of related molecules in organic solvents,<sup>[9a, 9g]</sup> we cannot really assign the new set of NMR signals to discrete  $c(\text{GC2})_4$  cyclic tetramers, since they are too broad and principally because fluorescence quenching, mainly attributable to stacked species, is quite pronounced within this intermediate  $V_{\text{THF}} = 0.3\text{--}0.1$  range (see Figure 2h). Instead, this picture is consistent with the formation of small aggregates by G:C H-bonding and stacking interactions that then grow as the water content is increased.

The morphology and size of the nanostructures formed by **GC2** in aqueous solutions were studied by AFM and TEM microscopies (Figures 3 and S2E-I).

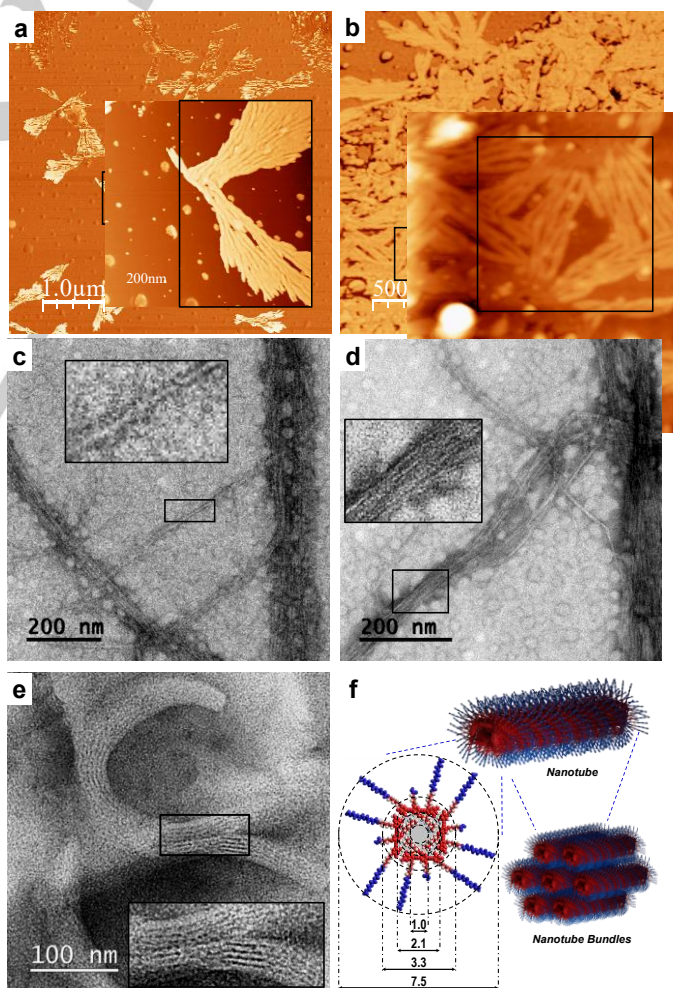


**Figure 3.** Microscopy measurements of **GC2** deposited from  $1.0\cdot 10^{-6}$ – $1.0\cdot 10^{-5}$  M  $\text{H}_2\text{O}$  or  $\text{MeOH}/\text{H}_2\text{O}$  solutions onto (a,b) HOPG and imaged by AFM, or (c–e) C-formvar Cu grids stained with phosphotungstic acid and imaged by TEM. (f) Nanotube models and dimensions. See Figures S2E–I and S2N for details.

## RESEARCH ARTICLE

In all cases, the presence of longitudinal objects was observed. Width dimensions obtained by TEM (Figures 3c-e and S2F-I), between 3 and 5 nm, matched rather well the outer diameter expected in our nanotube models (Figures 3f and S2N) and the dimensions of related lipophilic systems.<sup>[9]</sup> AFM profiles (see Figure S2E) showed nonetheless smaller height values, between 2 and 4 nm, which could be the result of the compression of side-chains by the force applied by the AFM probe,<sup>[12]</sup> and by the affinity of the assemblies for the surface. On the other hand, the tubular nature of the **GC2** assemblies was confirmed in stained samples measured by TEM (Figures 3c-d and S2F), in which nanotube walls presented darker contrast. In all cases, and in analogy with their lipophilic version,<sup>[9]</sup> the nanotubes displayed a large tendency to organize in aligned bundles, independently of sample preparation and experimental conditions.

The diameters measured by diverse microscopies and the NMR signals attributed to G:C pairing are decisive experimental evidence to propose a nanotube internal structure comprising a cyclic tetramer section, as depicted in Figures 1 and 3f. However, as mentioned before, the amphiphilic central block in **GC2** can alternate between two planar conformations that dispose either the lipophilic chiral alkyl tail or the hydrophilic carboxylate within the inner pore. It is expected that most central blocks will arrange with their lipophilic chains grouping within the pore and the carboxylates facing the external aqueous media, because the opposite conformation would lead to hydrophobic repulsion and to the accumulation of negatively charged groups in the pore. The relatively intense CD signals obtained already indicate the formation of ordered structures with a preferred helicity, due to the interaction between chiral chains, but additional evidence was sought to demonstrate a uniform lipophilic coating of the inner pore. Since, according to molecular models, the alkyl chains occupy less than 50% of the pore volume and they can in principle adapt different conformations, an indirect way to prove this would be to test the selective extraction and encapsulation of apolar molecules (*i.e.* insoluble in water) of appropriate size and chemical affinity for the nanotube pore. To this end, Nile Red (**NR**), which has been extensively used as a fluorescent hydrophobic probe for bilayer membranes, was tested (Figure 4a).<sup>[13]</sup>

In a very simple experiment for proving dye extraction, **GC2** ( $2.0 \cdot 10^{-4}$  M) and the **NR** dye ( $2.0 \cdot 10^{-5}$  M) were mixed in water. The spectroscopic features of this mixture were then compared with control samples of **GC2** and **NR** alone in the same experimental conditions by CD, absorption, emission (selectively exciting **NR** at 588 nm or **GC2** at 390 nm), and excitation measurements (Figures 4b-e). All these experiments indicate that **NR** is solubilized in the aqueous **GC2** solution by encapsulation within the lipophilic nanotube pores. **NR** is insoluble in water and absorption and emission in this medium is extremely weak. However, as shown in Figures 4b,c, an increase in the absorption (500-650 nm) and emission (600-750 nm) features of **NR** was observed when mixed with **GC2**. Moreover, the blue-shifted **NR** emission maximum (from 656 to 640 nm; Figure 4c) is characteristic of this solvatochromic probe when surrounded by apolar environments.<sup>[14]</sup> On the other hand, Figure 4d shows that **GC2** emission is quenched by a factor of 2 in the presence of **NR** and, interestingly, **NR** emission is concomitantly observed when **GC2** is excited in the mixture. This suggests the occurrence of an energy transfer process from **GC2** to the **NR** probe, which was confirmed in excitation experiments (Figure S4B), and thus that these two molecules are in close proximity. The efficiency of this

process in these conditions was calculated as 75%. Finally, the CD spectrum of the **GC2** nanotubes maintains the same Cotton effect, but the intensity is reduced in the presence of **NR** (Figure 4e). This might be explained taking into account that the inclusion of guest molecules in the tube pore would necessarily require a rearrangement of the lipophilic chains and hinder the interaction between chiral groups. It should be noted that these results are reproducible at different overall concentrations, down to  $10^{-5}$  M (see Figure S4A), and host:guest ratios, as explained below.

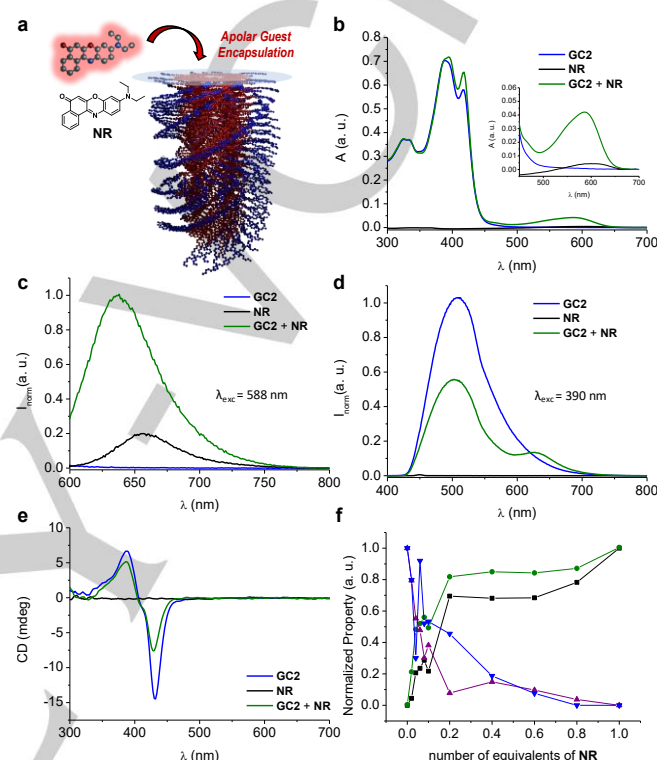


**Figure 4.** (a) Chemical structure of Nile Red (**NR**) and schematic illustration of its encapsulation inside **GC2** nanotubes. (b) Absorption, (c,d) emission at (c)  $\lambda_{\text{exc}} = 588$  nm and (d) 390 nm, and (e) CD spectra of **GC2** ( $2 \cdot 10^{-4}$  M; in blue), **NR** ( $2 \cdot 10^{-5}$  M; in black) and a mixture of **GC2** ( $2 \cdot 10^{-4}$  M) and **NR** ( $2 \cdot 10^{-5}$  M); in green) in Milli-Q water ( $l = 1$  mm for b,e and  $l = 1$  cm for c,d). The inset in (b) corresponds to the zoom in the dye absorption area. (f) Evolution of the spectra intensity of **GC2** when mixed with different amounts of **NR** in water. Black squares correspond to **NR** absorption at 588 nm, green circles to **NR** emission at 640 nm ( $\lambda_{\text{exc}} = 588$  nm), purple triangles to **GC2** emission at 507 nm ( $\lambda_{\text{exc}} = 390$  nm), and blue triangles to **GC2** CD signal at 424 nm. Lines are meant to guide the eye. See Figure S4C for all spectra and more details.

In order to determine the stoichiometry of the extraction process, and to see if it is consistent with our hypothesis, we performed titrations with increasing amounts of **NR** onto a  $1.0 \cdot 10^{-4}$  M water solution of **GC2**, and monitored CD, absorption and emission changes (exciting again each component separately at 390 or 588 nm). All spectra are shown in Figure S4C, whereas the titration trends are displayed in Figure 4f. All techniques seem to indicate that saturation, or the maximum encapsulation efficiency, is reached at around 0.2 equivalents of **NR** per molecule of **GC2**, and further **NR** addition produced little change in each of the corresponding spectra. In other words, a maximum of about 5 **GC2** molecules are able to host 1 **NR** molecule, which may indicate that the dye is inserted in between cyclic tetramer sections. Actually, **NR** extraction can already be seen by the



## RESEARCH ARTICLE

naked eye (Figure S4C). The initial clear pale yellow **GC2** solutions progressively acquire a greenish color below 0.2 **NR** equivalents, and further addition results in darker suspensions that, when centrifuged, reveal a **NR** precipitate at the bottom.

## Conclusion

In summary, in this work we made use of a bioinspired strategy that consists in shielding directional H-bonding interactions from the competing aqueous environment, to endow amphiphile assemblies with an accurate size and shape. Our novel design relies on amphiphilic monomers programmed with tailored lipophilic and hydrophilic sections and with complementary nucleobases at the edges. Their spontaneous organization in water yields a unique class of helically chiral micelle nanotubes with uniform, partially occupied lipophilic pores of about 2 nm in diameter. Importantly, these internal dimensions are not frequently realized with other types on nanotubes, and match rather well the scale of most molecules. As a result, our self-assembled nanotubes are able to extract and encapsulate guest molecules that are compatible in size and chemical affinity.

Moreover, although not demonstrated in this work, this novel amphiphile design potentially allows for a high structural, and thus functional, versatility. Nanotube stability might be enhanced by increasing the area of the hydrophobic sections. Pore diameter could be increased or decreased with subnanometer precision by tuning the length of the  $\pi$ -conjugated central block. Additionally, specific chemical functions could be incorporated in the lipophilic pore, which may open the door to the selective encapsulation and catalytic transformation of apolar molecules in confined nanospaces. These and other research directions will be the focus of future work.

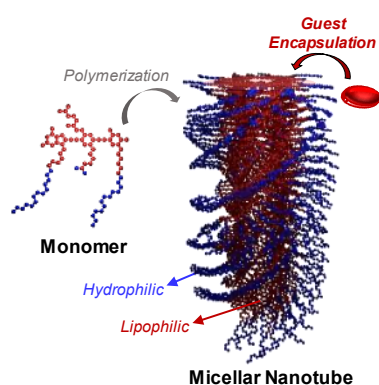
## Acknowledgements

Funding from the European Research Council (ERC-Starting Grant 279548 PROGRAM-NANO) and MINECO (CTQ2014-57729-P and CTQ2017-84727-P) is gratefully acknowledged. F.A. is grateful to MSCA-COFUND InterTalentum (713366) and MSCA-IF (793506) programs. P.B.C. acknowledges the Comunidad de Madrid for the PEJ-2017-AI/IND-6246 contract.

**Keywords:** Supramolecular Chemistry, Supramolecular Polymerization, Self-assembled Nanotubes, Amphiphiles.

- [1] a) G. V. Oshovsky, D. N. Reinhoudt, W. Verboom, *Angew. Chem., Int. Ed.* **2007**, *46*, 2366-2393; b) J. M. Zayed, N. Nouvel, U. Rauwald, O. A. Scherman, *Chem. Soc. Rev.* **2010**, *39*, 2806-2816; c) E. Krieg, B. Rybtchinski, *Chem. Eur. J.* **2011**, *17*, 9016-9026; d) Z. Laughrey, B. C. Gibb, *Chem. Soc. Rev.* **2011**, *40*, 363-386; e) P. S. Cremer, A. H. Flood, B. C. Gibb, D. L. Mobley, *Nat. Chem.* **2018**, *10*, 8-16.
- [2] T. Rehm, C. Schmuck, *Chem. Commun.* **2008**, 801-813.
- [3] a) C. Wang, Z. Wang, X. Zhang, *Acc. Chem. Res.* **2012**, *45*, 608-618; b) M. Ramanathan, L. K. Shrestha, T. Mori, Q. Ji, J. P. Hill, K. Ariga, *Phys. Chem. Chem. Phys.* **2013**, *15*, 10580-10611; c) N. Kundu, D. Banik, N. Sarkar, *Langmuir* **2018**, *34*, 11637-11654; d) S. I. Stupp, L. C. Palmer, *Chem. Mater.* **2014**, *26*, 507-518.
- [4] a) R. Chapman, M. Danial, M. L. Koh, K. A. Jolliffe, S. Perrier, *Chem. Soc. Rev.* **2012**, *41*, 6023-6041; b) J. Montenegro, M. R. Ghadiri, J. R. Granja, *Acc. Chem. Res.* **2013**, *46*, 2955-2965; c) B. Gong, Z. Shao, *Acc. Chem. Res.* **2013**, *46*, 2856-2866; d) L. S. Shimizu, S. R. Salpage, A. A. Korous, *Acc. Chem. Res.* **2014**, *47*, 2116-2127; e) A. Nitti, A. Pacini, D. Pasini, *Nanomaterials* **2017**, *7*, 167.
- [5] a) R. L. Beingessner, Y. Fan, H. Fenniri, *RSC Adv.* **2016**, *6*, 75820-75838; b) B. Adhikari, X. Lin, M. Yamauchi, H. Ouchi, K. Aratsu, S. Yagai, *Chem. Commun.* **2017**, 53, 9663-9683.
- [6] C.-Z. Liu, M. Yan, H. Wang, D.-W. Zhang, Z.-T. Li, *ACS Omega* **2018**, *3*, 5165-5176.
- [7] a) T. Shimizu, M. Masuda, H. Minamikawa, *Chem. Rev.* **2005**, *105*, 1401-1444; b) W. Zhang, W. Jin, T. Fukushima, A. Saeki, S. Seki, T. Aida, *Science* **2011**, *334*, 340-343; c) T. Shimizu, *Bull. Chem. Soc. Jpn.* **2018**, *91*, 623-668.
- [8] M. J. Mayoral, C. Montoro-García, D. González-Rodríguez, in *Comprehensive Supramolecular Chemistry II*, Elsevier, Oxford, **2017**, pp. 191-257.
- [9] a) C. Montoro-García, J. Camacho-García, A. M. López-Pérez, N. Bilbao, S. Romero-Pérez, M. J. Mayoral, D. González-Rodríguez, *Angew. Chem., Int. Ed.* **2015**, *54*, 6780-6784; b) C. Montoro-García, J. Camacho-García, A. M. López-Pérez, M. J. Mayoral, N. Bilbao, D. González-Rodríguez, *Angew. Chem., Int. Ed.* **2016**, *55*, 223-227; c) N. Bilbao, I. Destoop, S. De Feyter, D. González-Rodríguez, *Angew. Chem., Int. Ed.* **2016**, *55*, 659-663; d) C. Montoro-García, M. J. Mayoral, R. Chamorro, D. González-Rodríguez, *Angew. Chem., Int. Ed.* **2017**, *56*, 15649-15653; e) C. Montoro-García, N. Bilbao, I. M. Tsagri, F. Zaccaria, M. J. Mayoral, C. Fonseca Guerra, D. González-Rodríguez, *Chem. Eur. J.* **2018**, *24*, 11983-11991; f) M. J. Mayoral, D. Serrano-Molina, J. Camacho-García, E. Magdalena-Estirado, M. Blanco-Lomas, E. Fadaei, D. González-Rodríguez, *Chem. Sci.* **2018**, *9*, 7809-7821; g) V. Vázquez-González, M. J. Mayoral, R. Chamorro, M. M. R. M. Hendrix, I. K. Voets, D. González-Rodríguez, *J. Am. Chem. Soc.* **2019**, *141*, 16432-16438.
- [10] H. M. M. ten Eikelder, A. J. Markvoort, T. F. A. de Greef, P. A. J. Hilbers, *J. Phys. Chem. B* **2012**, *116*, 5291-5301.
- [11] P. A. Korevaar, C. Schaefer, T. F. A. de Greef, E. W. Meijer, *J. Am. Chem. Soc.* **2012**, *134*, 13482-13491.
- [12] M. A. Beuwer, M. F. Knopper, L. Albertazzi, D. van der Zwaag, W. G. Ellenbroek, E. W. Meijer, M. W. J. Prins, P. Zijlstra, *Polym. Chem.* **2016**, *7*, 7260-7268.
- [13] a) P. Greenspan, S. D. Fowler, *J. Lipid Res.* **1985**, *26*, 781-789; b) T. Delmas, A. Fraichard, P.-A. Bayle, I. Texier, M. Bardet, J. Baudry, J. Bibette, A.-C. Couffin, *J. Colloid Sci. Biotechnol.* **2012**, *1*, 16-25; c) S. Gupta, R. Tyagi, V. S. Parmar, S. K. Sharma, R. Haag, *Polymer* **2012**, *53*, 3053-3078.
- [14] a) S. Prasad, K. Achazi, C. Bottcher, R. Haag, S. K. Sharma, *RSC Adv.* **2017**, *7*, 22121-22132; b) S. Guo, Y. Song, Y. He, X.-Y. Hu, L. Wang, *Angew. Chem., Int. Ed.* **2018**, *57*, 3163-3167; c) C. M. A. Leenders, L. Albertazzi, T. Mes, M. M. E. Koenigs, A. R. A. Palmans, E. W. Meijer, *Chem. Commun.* **2013**, 49, 1963-1965; d) D. Janeliunas, R. Eelkema, B. Nieto-Ortega, F. J. Ramírez Aguilar, J. T. López Navarrete, L. van der Mee, M. C. A. Stuart, J. Casado, J. H. van Esch, *Org. Biomol. Chem.* **2013**, *11*, 8435-8442; e) M. Garzoni, M. B. Baker, C. M. A. Leenders, I. K. Voets, L. Albertazzi, A. R. A. Palmans, E. W. Meijer, G. M. Pavan, *J. Am. Chem. Soc.* **2016**, *138*, 13985-13995; f) M. H. Bakker, C. C. Lee, E. W. Meijer, P. Y. W. Dankers, L. Albertazzi, *ACS Nano* **2016**, *10*, 1845-1852.

## Entry for the Table of Contents



**Shaping amphiphile assemblies** into a novel class of tubular architectures has been realized by programming an unconventional amphiphilic molecule with directional Watson-Crick hydrogen-bonding interactions that are shielded from the aqueous environment. These self-assembled nanotubes are endowed with chiral lipophilic pores of about 2 nm in diameter that are able to encapsulate molecules that are complementary in size and chemical affinity.

Researcher Twitter usernames: @DGRlab

Institute Twitter username: @UOrganicchem